Science Advances
AAAS

advances.sciencemag.org/cgi/content/full/7/8/eabc4631/DC1

Supplementary Materials for

Do photosynthetic complexes use quantum coherence to increase their efficiency? Probably not

Elinor Zerah Harush and Yonatan Dubi*

*Corresponding author. Email: jdubi@bgu.ac.il

Published 17 February 2021, *Sci. Adv.* **7**, eabc4631 (2021)
DOI: 10.1126/sciadv.abc4631

This PDF file includes:

I. DETAILED DESCRIPTION OF THE COMPUTATIONAL PROCEDURE: LINDBLAD EQUATION AND ETC HAMILTONIANS.

We start by describing the system under study by a general Hamiltonian,

$$H = H_S + H_B + H_{SB} \ , \tag{S1}$$

where we divide the system into three parts: The ETC itself (the "reduced system" H_S, see detailed Hamiltonians of the natural systems in Sec. VI of this SM), the protein and the molecular vibrations i.e phonons, (addressed here as the "bath", H_B) and the interaction between them (H_{SB}). H_B describes the environment, which in fact includes three different bathes: the antenna, the reaction center, and the phonon (vibration) bath. H_{SB} is the interaction Hamiltonian that depicts the interaction between the bath and the reduced system.
The system dynamics are described by the Lindblad equation (e.g., ref 43):

$$\frac{d\rho_S}{dt} = -i[H_S, \rho_S] + L\rho_s \ \ , \tag{S2}$$

where ρ_S is the density matrix of the reduced system and L is the Lindblad-operator, defined as:

$$L\rho_s = \sum_k \gamma_k \big(V_k \rho_S V_k^\dagger - \frac{1}{2}\{V_k^\dagger V_k, \rho_S\}\big) \ \ , \tag{S3}$$

where V_k are Lindblad operators describing the action of the environment on the system, and γ_k is the respective rate of the Lindblad operator.
In the presence of multiple environments - source, drain and dephasing environments

- the Lindblad equation has the form of:

$$\frac{d\rho}{dt} = -i[H,\rho] + L_{inj}\rho + L_{ext}\rho + L_{dep}\rho \ . \tag{S4}$$

$L_{inj}\rho$, $L_{ext}\rho$ and $L_{dep}\rho$ are the injection, extraction and dephasing elements, respectively, with the corresponding Lindblad operators $V_{inj} = \sqrt{\gamma_{inj}}a^{\dagger}_{inj}$, $V_{ext} = \sqrt{\gamma_{ext}}a_{ext}$ describing creation and anihilation of an exciton in the injection and extraction sites. The dephasing operator is $V_{dep} = \sqrt{\gamma_{dep}}\sum_i a^{\dagger}_i a_i$.

Following the steps detailed in Ref. 38, one finds for the exciton current is given by :

$$J_p = \mathrm{Tr}(\langle n\rangle L_{ext}) = \gamma_{ext}\rho_{n,n} \ , \tag{S5}$$

Where $\langle n\rangle$ is the occupation matrix.

II. ANALYTIC DESCRIPTION OF ENAQT

Using equations S2-S5, here we analyse a simple system of three sites, with excitation from site 1 and extraction site 2. The elements of the Lindbladian are given by:

$$\begin{aligned} -i[H_3,\rho] = -i\Bigg(\sum_{i=1}^{3} \epsilon_i \big(\rho_{i,0}|\psi_i\rangle\langle\psi_0| - \rho_{0,i}|\psi_0\rangle\langle\psi_i|\big) + \sum_{m,l=1}^{3} (\epsilon_m - \epsilon_3)\rho_{m,l}|\psi_m\rangle\langle\psi_l| \\ + \sum_{m,l,i}^{2} t_{(i,i+1)}\rho_{(i+1,i)}|\psi_i\rangle\langle\psi_l| - \sum_{j}^{2} t_{(j+1,j)}\rho_{(j,j+1)}|\psi_m\rangle\langle\psi_j|\Bigg) \ , \end{aligned} \tag{S6}$$

$$L_{inj}\rho = \gamma_{inj}\Big[|\langle\psi_1\rangle\langle\psi_1|\rho_{0,0} - \frac{1}{2}\sum_{m=0}^{3}\rho_{0,m}|\psi_0\rangle\langle\psi_m| - \frac{1}{2}\sum_{m=0}^{3}\rho_{m,0}|\psi_m\rangle\langle\psi_0|\Big] \ , \tag{S7}$$

$$L_{ext}\rho = \gamma_2\Big[|\langle\psi_0\rangle\langle\psi_0|\rho_{2,2} - \frac{1}{2}\sum_{m=0}\rho_{2,m}|\psi_2\rangle\langle\psi_m| - \frac{1}{2}\sum_{m=0}^{n}\rho_{m,2}|\psi_m\rangle\langle\psi_2|\Big] \ , \tag{S8}$$

$$L_{dep}\rho = \gamma_{dep}\sum_{u}^{3}\Big[|\psi_u\rangle\langle\psi_u|\rho_{u,u} - \frac{1}{2}\sum_{m}\rho_{u,m}|\psi_u\rangle\langle\psi_m| - \frac{1}{2}\sum_{m}\rho_{u,m}|\psi_m\rangle\langle\psi_u|\Big] \ . \tag{S9}$$

i, j are indexes for an unspecific position in the system. The index 0 refers to the empty state (a system with zero excitons). γ_{inj},γ_{ext} and γ_{dep} are the excitation, extraction and dephasing rates, respectively. Replacing $L_{ext}, L_{inj}, L_{dep}, -i[H,\rho]$ in S4 with the terms from equations S6-S7 and using equation S5 we find and expression for the current:

$$J_p = \frac{2t^2\gamma_{deph}\alpha}{\gamma_{deph}^2\alpha + \frac{1}{2}\gamma_{deph}\gamma_{inj} + 2t^2\alpha + \frac{6t^2\gamma_{deph}\alpha^2}{\gamma_{inj}} + \frac{2t^2\gamma_{deph}\alpha}{\gamma_{inj}}} \tag{S10}$$

where $\alpha = \frac{\gamma_{inj}}{\gamma_{ext}}$. The current is non-monotonic in dephasing rate, with maximum current at

$$\gamma_{dep,mx} = \sqrt{2}t \ \ . \tag{S11}$$

This result can be generalized to $\gamma_{dep,mx} \sim \bar{t}$ in systems of non-uniform couplings, where $\bar{t}$ is an effective coupling constant that depends on the systems geometry and/or hopping matrix elements distribution. From Eq. S10 we can also extract the regimes for the onset of ENAQT and onset of classicality. To find the onset of ENAQT, we note that at small dephasing rate, the current is always linear in γ_{deph}. The deviation from linearity can thus serve as an indicator for the deviation from the quantum regime to the ENAQT regime. From an expansion to the third order in γ_{deph} (the second order term is always negative) and examining the deviation from linearity, we find (at the limit of small α) $\gamma_{deph,1} \approx \gamma_{inj}$. In a similar way, we can find the onset of classicality. In the classical regime, current is proportional to γ_{deph}^{-1}. The deviation form this behavior can be found by expanding J_p in powers of γ_{deph}^{-1}. Again

comparing the 1st and 3rd orders we find $\gamma_{deph,2} \approx \frac{2t^2}{\gamma_{inj}} + \frac{4t^2}{\gamma_{ext}} + \gamma_{ext}/2$. The onset of classicality is then the maximal of the these three elements, which for physiological parameters is $\frac{2t^2}{\gamma_{inj}}$. These analytics can be summarized by the approximate relation describing the range of ENAQT,

$$\gamma_{inj} \lesssim \gamma_{deph} \lesssim \frac{2t^2}{\gamma_{inj}} \ , \quad \gamma_{deph,mx} \sim \sqrt{t} \ . \tag{S12}$$

III. ENAQT ENHANCEMENT AT THE EXTREME PARAMETER RANGE

In the main text we evaluate the physiological injection and extraction rates. Here we show that even if these restrictions are released (allowing for, e.g. an enhancement of the injection rate, which is the central limiting factor for current), still there is only a minor enhancement of current in the ENAQT regime compared to the quantum regime. In Fig. S1 we plot the current enhancement (ratio between maximal current in the ENAQT regime and current at zero dephasing) as a function of injection and extraction rates, going beyond the limits of physiological conditions. We find that the enhancement is linear in γ_{inj} but seems to be quadratic in γ_{ext}. In both FMO and PC-645, even when pushing parameter regime to extremely large values (very slow extraction and very high injection rates) the enhancement of the ENAQT regime reaches only a few percent.

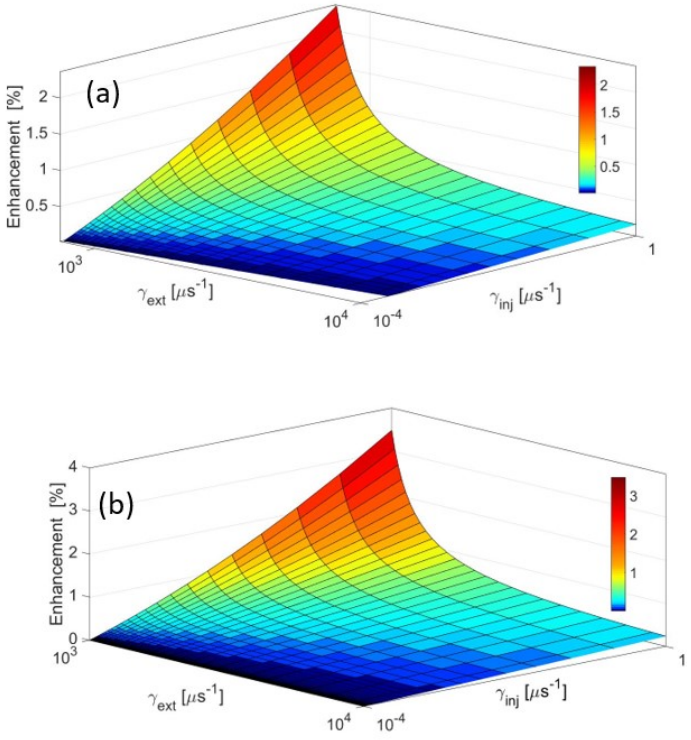

FIG. S1. Current enhancement as a function of injection (γ_{inj}) and extraction (γ_{ext}) rates for FMO (a) and pc-645 (b).The enhancement was taken for the estimated biologic dephasing rate ($\gamma_{deph} \approx 10^6 \mu s^{-1}$). Maximum enhancement that can be achieved is $\approx 3\%$, which is obtained for extreme conditions that are almost impossible in natural process

IV. MULTIPLE EXCITATIONS AND INJECTIONS IN LH2

The physiological Excitation rate of LH2 is estimated as $\gamma_{inj} \approx 10^{-4}\mu s^{-1}$, which is much lower than the extraction site. Thus, it can be safely assumed that typically there is only one exciton excited in the system (or two in extreme cases). However, in order to strengthen our claim, we evaluate the current in the case of multiple (two or three) excitations (and up to four exciton extraction sites). Figure S2 (inset) shows the current as a function of dephasing rates for an arbitrary set of selected configurations with different injection and extraction sites. The behavior is similar to that described in the main text, namely a convergence of all the currents in the ENAQT regime. The main panel of figure S2 shows a histogram of the ENAQT enhancement from $10,000$ different configurations that can occur on LH2 (different position and number of injection and extraction sites). We find that only a marginal number of configurations have enhancement of more than 2 percent.

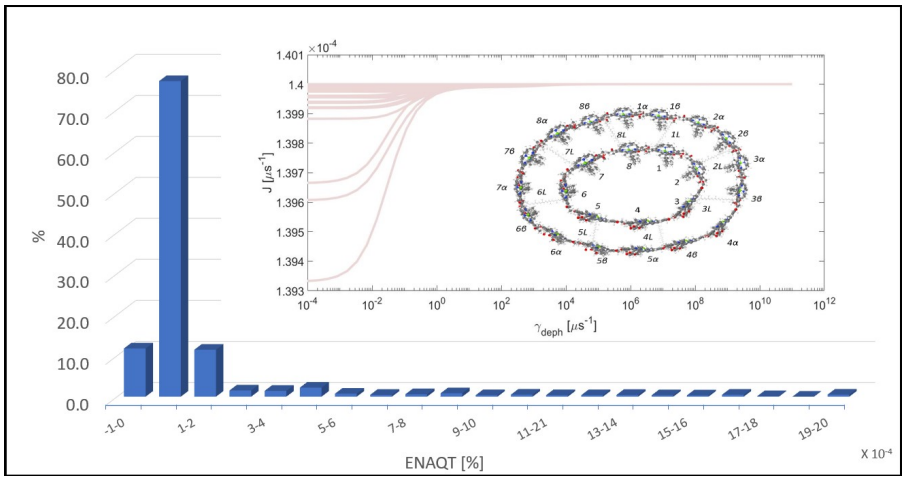

FIG. S2. Histogram of current enhancement from 10,000 different configurations of injection and extraction sites. In the inset: Pink curves shows the particle current of arbitrary configurations of excitation and extraction sites. The differences are minor, and derived from the different geometry formed by injection/extraction sites.

V. EXCITATION IN THE ENERGY BASIS

In order to verify that there are no conditions that allow a significant enhancement of current from the quantum to the ENAQT regimes, we study the ENAQT created from excitation in the energy basis of LH2. We repeat the calculation described in the main text for the LH2 complex, but instead of using an excitation operator which is localized in a specific site, is in localized in an energy eigenvector; we start by diagonalizing the LH2 Hamiltonian $\mathcal{H}_{LHII}$. The single-particle eigenvectors $|\psi_n\rangle = \sum_i \psi_n(i)|i\rangle$ (where $|i\rangle$ are localized orbitals) are then used to construct Lindblad injection operators, $V_{inj,n} = \sum_i \psi_n(i) a_i^\dagger$, where n is the eigenstate index. Figure S3 shows the particle current of selected examples of different excitation level (i.e. different ns) and extraction sites. The inset presents the histogram of all possibilities.

The maximum enhancement is 0.46%, which is obtained for only 3 configurations, the average is much smaller (0.03%), showing that ENAQT has a negligible influence on the current. Again, in the ENAQT regime all curves converge.

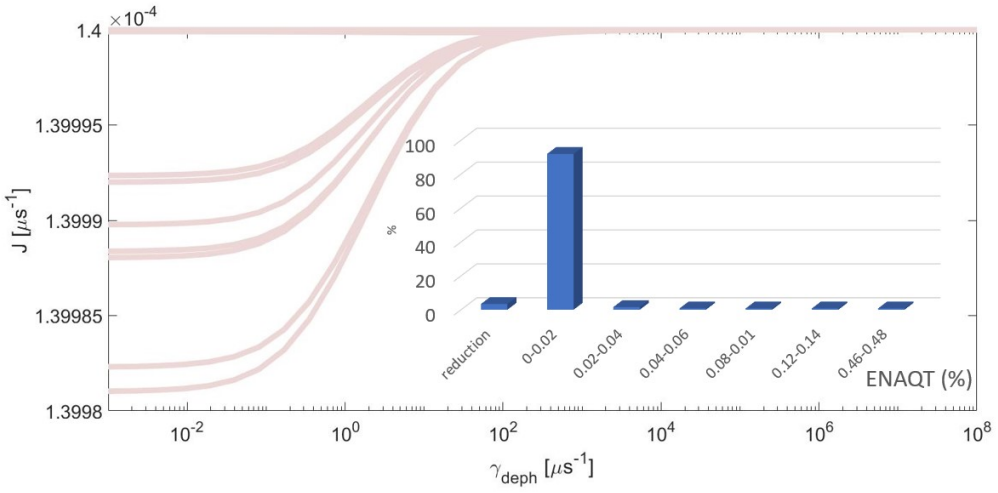

FIG. S3. Current as a function of dephasing rate for the case for excitation in the energy basis. Pink curves show the current for several selected eigenbasis excitations (see text). (inset) Histogram for the enhancement obtained from excitation of each energy level and each extraction site.

VI. DETAILED HAMILTONIAN

Hamiltonian matrices that were used in our calculations are (in cm^{-1}):

FMO Hamilonian (49)

$$H_{FMO} = \begin{pmatrix} 12335 & -106 & 8 & -5 & 6 & -8 & -4 \\ -106 & 12475 & 28 & 6 & 2 & 13 & 1 \\ 8 & 28 & 12055 & -62 & -1 & -9 & 17 \\ -5 & 6 & -62 & 12230 & -70 & -19 & -57 \\ 6 & 2 & -1 & -70 & 12375 & 40 & -2 \\ -8 & 13 & -9 & -19 & 40 & 12415 & 32 \\ -4 & 1 & 17 & -57 & -2 & 32 & 12315 \end{pmatrix} \tag{S13}$$

Pc-645 Hamiltonian (53)

$$H_{pc645} = \begin{pmatrix} 17034 & 319.4 & -9.6 & -43.9 & 20.3 & 25.3 & -46.8 & -20 \\ 319.4 & 17116 & 43.9 & 7.7 & 30.5 & 29 & 21.5 & 48 \\ -9.6 & 43.9 & 16050 & 4.3 & -86.7 & -2.9 & -15.8 & 49.3 \\ -43.9 & 7.7 & 4.3 & 16373 & 3.4 & 86.2 & 53.8 & -14.7 \\ 20.3 & 30.5 & -86.7 & 3.4 & 15808 & 7.8 & 11 & 10 \\ 25.3 & 29 & -2.9 & 86.2 & 7.8 & 15889 & 29 & -10.7 \\ -46.8 & 21.5 & -15.8 & 53.8 & 11 & 29 & 15566 & 48 \\ -20 & 48 & 49.3 & -14.7 & 10 & -10.7 & 48 & 15647 \end{pmatrix} \tag{S14}$$

LH2 Hamiltonian (51,52)

$$H_{LH2} = \begin{pmatrix} H_{B850\alpha} & H_c(B_{850\alpha}, B_{850\beta}) & H_c(B_{850\alpha}, B_{800}) & H_c(B_{850\alpha}, B_{Lyco} \\ H_c(B_{850\beta}, B_{850\alpha}) & H_{B850\beta} & H_c(B_{850\beta}, B_{800}) & H_c(B_{850\beta}, B_{Lyco}) \\ H_c(B_{800}, B_{850\alpha}) & H_c(B_{800}, B_{850\beta}) & H_{B800} & H_c(B_{800}, B_{Lyco}) \\ H_c(B_{Lyco}, B_{850\alpha}) & H_c(B_{Lyco}, B_{850\beta}) & H_c(B_{Lyco}, B_{B800}) & H_{Lyco} \end{pmatrix} \tag{S15}$$

where $H_c(H_i, H_j) = H_c(H_j, H_i)$ are the coupling between H_i and H_j.

Hamiltonian are given here:

$$H_{B850\alpha} = \begin{pmatrix} 12826.53 & -67 & 0 & 0 & 0 & 0 & 0 \\ -67 & 12826.53 & -67 & 0 & 0 & 0 & 0 \\ 0 & -67 & 12826.53 & -67 & 0 & 0 & 0 \\ 0 & 0 & -67 & 12826.53 & -67 & 0 & 0 \\ 0 & 0 & 0 & -67 & 12826.53 & -67 & 0 \\ 0 & 0 & 0 & 0 & -67 & 12826.53 & -67 \\ 0 & 0 & 0 & 0 & 0 & -67 & 12826.53 \end{pmatrix} \tag{S16}$$

$$H_{B850\beta} = \begin{pmatrix} 12826.53 & -40 & 0 & 0 & 0 & 0 & 0 & -40 \\ -40 & 12987.87 & -40 & 0 & 0 & 0 & 0 & 0 \\ 0 & -40 & 12987.87 & -40 & 0 & 0 & 0 & 0 \\ 0 & 0 & -40 & 12987.87 & -40 & 0 & 0 & 0 \\ 0 & 0 & 0 & -40 & 12987.87 & -40 & 0 & 0 \\ 0 & 0 & 0 & 0 & -40 & 12987.87 & -40 & 0 \\ 0 & 0 & 0 & 0 & 0 & -40 & 12987.87 & -40 \\ -40 & 0 & 0 & 0 & 0 & 0 & -40 & 12987.87 \end{pmatrix} \tag{S17}$$

$$H_{B800} = \begin{pmatrix} 12584.52 & -19 & -3.6 & 0 & 0 & 0 & -3.6 & -19 \\ -19 & 12584.52 & -19 & -3.6 & 0 & 0 & 0 & -3.6 \\ -3.6 & -19 & 12584.52 & -19 & -3.6 & 0 & 0 & 0 \\ 0 & -3.6 & -19 & 12584.52 & -19 & -3.6 & 0 & 0 \\ 0 & 0 & -3.6 & -19 & 12584.52 & -19 & -3.6 & 0 \\ 0 & 0 & 0 & -3.6 & -19 & 12584.52 & -19 & -3.6 \\ -3.6 & 0 & 0 & 0 & -3.6 & -19 & 12584.52 & -19 \\ -19 & -3.6 & 0 & 0 & 0 & -3.6 & -19 & 12584.52 \end{pmatrix} \tag{S18}$$

$$H_{Lyco} = \begin{pmatrix} 21942.24 & 89 & 8.7 & 0 & 0 & 0 & 0 & 8.7 & 89 \\ 89 & 21942.24 & 89 & 8.7 & 0 & 0 & 0 & 0 & 8.7 \\ 8.7 & 89 & 21942.24 & 89 & 8.7 & 0 & 0 & 0 & 0 \\ 0 & 8.7 & 89 & 21942.24 & 89 & 8.7 & 0 & 0 & 0 \\ 0 & 0 & 8.7 & 89 & 21942.24 & 89 & 8.7 & 0 & 0 \\ 0 & 0 & 0 & 8.7 & 89 & 21942.24 & 89 & 8.7 & 0 \\ 0 & 0 & 0 & 0 & 8.7 & 89 & 21942.24 & 89 & 8.7 \\ 8.7 & 0 & 0 & 0 & 0 & 8.7 & 89 & 21942.24 & 89 \\ 89 & 8.7 & 0 & 0 & 0 & 0 & 8.7 & 89 & 21942.24 \end{pmatrix} \tag{S19}$$

$$H_c(H_{B850\alpha}, H_{B850\beta}) = \begin{pmatrix} 258 & 22 & 0 & 0 & 0 & 17 & 210 \\ 210 & 258 & 22 & 0 & 0 & 0 & 17 \\ 17 & 210 & 258 & 22 & 0 & 0 & 0 \\ 0 & 17 & 210 & 258 & 22 & 0 & 0 \\ 0 & 0 & 17 & 210 & 258 & 22 & 0 \\ 0 & 0 & 0 & 17 & 210 & 258 & 22 \\ 22 & 0 & 0 & 0 & 17 & 210 & 258 \end{pmatrix} \tag{S20}$$

$$H_c(H_{B850\alpha}, H_{B800}) = \begin{pmatrix} 8.2 & 0 & 0 & 0 & 0 & 0 & 0 & -36 \\ -36 & 8.2 & 0 & 0 & 0 & 0 & 0 & 0 \\ 0 & -36 & 8.2 & 0 & 0 & 0 & 0 & 0 \\ 0 & 0 & -36 & 8.2 & 0 & 0 & 0 & 0 \\ 0 & 0 & 0 & -36 & 8.2 & 0 & 0 & 0 \\ 0 & 0 & 0 & 0 & -36 & 8.2 & 0 & 0 \\ 0 & 0 & 0 & 0 & 0 & -36 & 8.2 & 0 \\ 0 & 0 & 0 & 0 & 0 & 0 & -36 & 8.2 \end{pmatrix} \tag{S21}$$

$$H_c(H_{B850\alpha}, H_{Lyco}) = \begin{pmatrix} -50 & -2.3 & 0 & 0 & 0 & 16 & 49 & 96 \\ 96 & -50 & -2.3 & 0 & 0 & 0 & 16 & 49 \\ 49 & 96 & -50 & -2.3 & 0 & 0 & 0 & 16 \\ 16 & 49 & 96 & -50 & -2.3 & 0 & 0 & 0 \\ 0 & 16 & 49 & 96 & -50 & -2.3 & 0 & 0 \\ 0 & 0 & 16 & 49 & 96 & -50 & -2.3 & 0 \\ 0 & 0 & 0 & 16 & 49 & 96 & -50 & -2.3 \\ -2.3 & 0 & 0 & 0 & 16 & 49 & 96 & -50 \end{pmatrix} \tag{S22}$$

$$H_c(H_{B850\beta}, H_{B800}) = \begin{pmatrix} 25 & 0 & 0 & 0 & 0 & 0 & 0 & 5.4 \\ 5.4 & 25 & 0 & 0 & 0 & 0 & 0 & 0 \\ 0 & 5.4 & 25 & 0 & 0 & 0 & 0 & 0 \\ 0 & 0 & 5.4 & 25 & 0 & 0 & 0 & 0 \\ 0 & 0 & 0 & 5.4 & 25 & 0 & 0 & 0 \\ 0 & 0 & 0 & 0 & 5.4 & 25 & 0 & 0 \\ 0 & 0 & 0 & 0 & 0 & 5.4 & 25 & 0 \\ 0 & 0 & 0 & 0 & 0 & 0 & 5.4 & 25 \end{pmatrix} \tag{S23}$$

$$H_c(H_{B850\beta}, H_{Lyco}) = \begin{pmatrix} 48 & 2.6 & 0 & 0 & 0 & 0 & -30 & -138 \\ -138 & 48 & 2.6 & 0 & 0 & 0 & 0 & -30 \\ -30 & -138 & 48 & 2.6 & 0 & 0 & 0 & 0 \\ 0 & -30 & -138 & 48 & 2.6 & 0 & 0 & 0 \\ 0 & 0 & -30 & -138 & 48 & 2.6 & 0 & 0 \\ 0 & 0 & 0 & -30 & -138 & 48 & 2.6 & 0 \\ 0 & 0 & 0 & 0 & -30 & -138 & 48 & 2.6 \\ 2.6 & 0 & 0 & 0 & 0 & -30 & -138 & 48 \end{pmatrix} \quad \text{(S24)}$$

$$H_c(H_{B800}, H_{Lyco}) = \begin{pmatrix} 65 & -78 & -16 & 0 & 0 & 0 & 0 & -18 \\ -18 & 65 & -78 & -16 & 0 & 0 & 0 & 0 \\ 0 & -18 & 65 & -78 & -16 & 0 & 0 & 0 \\ 0 & 0 & -18 & 65 & -78 & -16 & 0 & 0 \\ 0 & 0 & 0 & -18 & 65 & -78 & -16 & 0 \\ 0 & 0 & 0 & 0 & -18 & 65 & -78 & -16 \\ -16 & 0 & 0 & 0 & 0 & -18 & 65 & -78 \\ -78 & -16 & 0 & 0 & 0 & 0 & -1865 & \end{pmatrix} \quad \text{(S25)}$$